Journal of Alloys and Compounds 506 (2010) 51–56

Contents lists available at ScienceDirect

Journal of Alloys and Compounds

journal homepage: www.elsevier.com/locate/jallcom

Measurement and modelling of the characteristic parameters for silver Schottky contacts on layered *p*-GaSe compound in a wide temperature range

B. Abay*

Atatürk University, Faculty of Sciences, Department of Physics, 25240 Erzurum, Turkey

ARTICLE INFO

Article history:
Received 5 January 2010
Received in revised form 6 May 2010
Accepted 8 July 2010
Available online 21 July 2010

PACS:
73.30.+y
73.40.Qv
73.40.Ns

Keywords:
GaSe
Layered crystal
Crystal growth
Schottky diode
Temperature dependent *I–V* measurement
Double Gaussian distribution
Barrier inhomogeneities

ABSTRACT

The temperature dependent barrier characteristics of Ag/*p*-GaSe Schottky barrier diodes have been analyzed in the temperature range of 70–350 K based on thermionic emission (TE) theory. Barrier height (BH) (φ_{b0}), ideality factor (n) and serial resistance (R_s) have been found to be strongly temperature dependent. Decrease in the φ_{b0} and an increase in the n with decrease in temperature has been observed. The conventional Richardson plot exhibits non-linearity below 180 K with the linear portion corresponding to activation energy of 0.62 eV. The value of Richardson constant (A^*) turns out to be 5.15×10^{-4} A K^{-2} cm^{-2} against the theoretical value of 60 A K^{-2} cm^{-2} for *p*-GaSe. It has been demonstrated that these behaviors result from the spatial BH inhomogeneities prevailing at the metal–semiconductor interface. For the interpretation of the BH inhomogeneity, multiple Gaussian distribution model developed by Jiang et al. [1] has been used. Furthermore, an expression defining temperature dependent ideality factor has been derived for the diodes with spatial BH inhomogeneities considering multiple Gaussian distribution. The temperature dependent BH of the device has shown a Double Gaussian Distribution (DGD) having mean BH ($\bar{\varphi}_{b0}$) of 1.21 and 1.08 eV with standard deviations (σ_0) of 0.103 and 0.097 eV in the 180–350 and 70–180 K regions, respectively. $\bar{\varphi}_{b0}$ and A^* values have also been obtained as 1.209 eV, 62.8 A K^{-2} cm^{-2} and 1.097 eV, 56.8 A K^{-2} cm^{-2} from the modified Richardson plots for the respective temperature regions, respectively. These values of A^* are in close agreement with that of the known value for *p*-type GaSe. It has been shown that these results support the predictions of the multiple GD model of spatial BH inhomogeneities in the temperature range of 70–350 K.

1. Introduction

Gallium selenide (GaSe) belonging to $A^{III}B^{VI}$ semiconductor compounds has a layered structure and contains two atomic layers in the sequence of Se–Ga–Ga–Se per primitive cell [2]. The forces between adjacent layers are weak, predominantly of van der Waals type, whereas the intra-layer forces are of ionic-covalent type [2]. So, they can easily be cleaved across their van der Waals gap between the layers, which leads to the outer surfaces closely resembling the inner ones. Cleavage planes of the layered crystals have been found to be free of dangling bonds and proved very inert to chemical reactions. Therefore, the layered semiconductors may be considered as idealized substrates for the investigation of fundamental aspects of surface or interface reactions [3,4].

In a better understanding of electrical properties of any semiconductor material, it has great importance to be known its contact behavior with several other substances. The investigation of the metal–semiconductor (MS) contacts is of current interest for most elemental and compound semiconductors. MS contacts have many device applications such as the gate electrode of a field-effect transistor, the source and drain contacts in metal-oxide-semiconductor field-effect transistors (MOSFET) and the electrodes for high-power oscillators [5]. MS contact based devices are very sensitive to the electrical properties of MS interface and any mechanism that affects the interface influences the performance of these devices. Therefore, this highly productive characteristic of the MS structures can be merged with the surface and/or interface features of the layered crystals to obtain some useful knowledge for this area of the semiconductor technology. However, characterization of the Schottky barrier diodes (SBDs) only at the room temperature does not give detailed information about their conduction process or the nature of barrier formation at the MS interface. Hence, the temperature dependent electrical characterization allows us to understand the different aspects of conduction mechanisms of these devices.

Although the structural, electrical, optical absorption and photoelectric properties have been widely investigated [6–10], only a few reports have been published on the metal/*p*-GaSe SBDs [11–16]. In contrast to other layered semiconductors [17–21], to my knowledge, measurements and modelling of the characteristic parameters for silver SBDs fabricated on *p*-GaSe have not yet

* Tel.: +90 442 231 41 81; fax: +90 442 236 09 48.
E-mail address: babay@atauni.edu.tr.

0925-8388/$ – see front matter © 2010 Elsevier B.V. All rights reserved.
doi:10.1016/j.jallcom.2010.07.034

been reported. Therefore, it would be interesting to investigate the temperature dependence of Ag/*p*-GaSe SBD parameters such as the ideality factor (n), barrier height (BH) and serial resistance (R_s).

Thermionic emission (TE) theory is normally used to extract the SBD parameters [5,22–24]; however, there have been several reports of certain anomalies [25–27] at low temperatures. The ideality factor and BH determined from the forward *I–V* characteristics were found to be a strong function of temperature [28–34]. Generally, the ideality factor n was found to increase, while the BH decreases with decreasing temperature. The decrease in the BH at low temperatures leads to non-linearity in the conventional Richardson plot. These anomalies have been satisfactorily explained recently by incorporating the concept of BH inhomogeneities and introducing a TE mechanism with a Gaussian distribution (GD) function with a mean BH and a standard deviation for the description in some studies [35–41].

In this study, my novel results on the forward bias diode parameters of Ag/*p*-GaSe structure in the 70–350 K temperature range were presented. The temperature dependent barrier characteristics were analyzed and modelled by assuming multiple GD of the BHs based on TE theory.

2. Experimental procedure

Single crystals of unintentionally doped GaSe were grown by the Bridgman–Stockbarger method, from a stoichiometric melt of 6N Ga and 5N Se starting materials, obtained from Alfa Aesar, in a carbon coated and vacuum-sealed quartz ampoules with a tip at the bottom, in our crystal growth laboratory. Details of the experimental procedure for the crystal growth are reported elsewhere [42]. Growth crystals were found to be *p*-type by using the Hall Effect and thermal electromagnetic force (emf) methods.

The sample (with about $8 \times 8\,mm^2$ area and 100–200 μm thickness) was cut from the freshly cleaved sheets with a razor blade (no further polishing or cleaning treatments were required because of the natural mirror-like cleavage faces of the samples) and inserted into the deposition chamber immediately. Ohmic contact of low resistance on the front side of the sample was formed by evaporating of indium (In) followed by a temperature treatment at 300 °C for 5 min in nitrogen atmosphere. After peeling a thin layer from the back surface of the sample, it was inserted into the deposition chamber immediately and circular dots of 1.0 mm diameters silver (Ag) contacts were deposited onto the freshly cleaved back surface of the sample through a molybdenum shadow mask. The deposition process was carried out in the Leybold-Heraeus Univex 300 vacuum-coating unit under the pressure of less than 2×10^{-6} mbar.

The current–voltage (*I–V*) characteristics of the devices were measured by using a computer controlled Keithley 487 Picoammeter/Voltage Source, supported by a software program, in the temperature range of 70–350 K in the dark. The measurements below room temperature were performed by mounting the device onto the specially designed probe station on the cold finger of ARS HC-2 closed-cycle helium cryostat, which enables us to make measurements in the temperature range of 6–450 K. The device temperature was controlled within an accuracy of ±0.1 K by a Lake Shore 331 auto-tuning temperature controller.

3. Results and discussion

The forward *J–V* characteristics of most Schottky contacts based on the TE theory can be expressed as [5,22]:

$$J = J_0 \exp\left(\frac{qV_d}{nkT}\right)\left[1 - \exp\left(-\frac{qV_d}{kT}\right)\right], \quad (1)$$

with

$$J_0 = A^* T^2 \exp\left(-\frac{q\varphi_{b0}}{kT}\right). \quad (2)$$

where J_0 is the saturation current density, q is the electron charge, T is the absolute temperature, A^* is the effective Richardson constant, found to be $60\,A\,K^{-2}\,cm^{-2}$ for *p*-type GaSe from $A^* = 120 m_h^*$ where $m_h^* = (0.5 m_0)$ is the density-of-states effective mass in the valance band [43], k is the Boltzmann constant, V_d ($= V - A_{eff} R_s J$) is the voltage drop across the diode, A_{eff} is the effective area of the diode, φ_{b0} ($= \varphi_b(V=0)$) is the zero bias BH, n ($=1/(1-\beta)$) is the ideality factor and β ($= \partial\varphi_b/\partial V$) is the change in the BH with bias voltage. If β is constant, n is also constant. For the values of V greater than $3kT/q$. Eq. (1) can be written in the simpler form

$$J = J_0 \exp\left(\frac{qV_d}{nkT}\right), \quad (3)$$

so that a plot of $\ln J$ vs. V in the forward direction should give a straight line except for the region where $V < 3kT/q$ [22]. Hence, saturation current density J_0 is derived from the intercept of the straight line in the semi-logarithmic *J–V* plot for zero bias and the values of φ_{b0} and n of a SBD can be extracted from the intercept and the slope of the linear portion of the semi-logarithmic *J–V* plot, respectively, while the R_s data is deduced from the best fit of experimental *J–V* data in Eq. (3). But, Eq. (1) has the advantage that n can be found experimentally by plotting $\ln[J/\{1 - \exp(qV_d/kT)\}]$ vs. V_d. This plot should be a straight line of which slope q/nkT if n is constant, even for $V < 3kT/q$. However, more usually β is not constant and the plot of $\ln[J/\{1 - \exp(qV_d/kT)\}]$ vs. V_d is not linear. In this case,

$$\frac{1}{n} = \frac{kT}{q}\frac{d}{dV}\ln\left[\frac{J}{1 - \exp(qV_d/kT)}\right] \quad (4)$$

or, for $V > 3kT/q$,

$$\frac{1}{n} = \frac{kT}{q}\frac{d(\ln J)}{dV}. \quad (5)$$

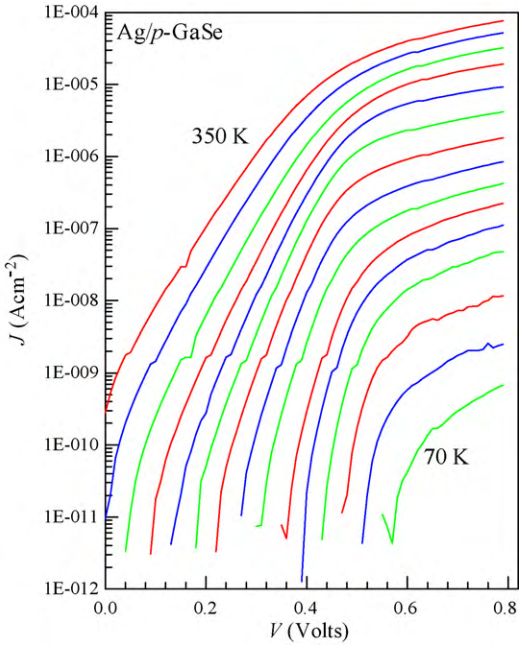

Fig. 1. Experimental forward bias *J–V* characteristics of a typical Ag/*p*-GaSe SBD in the temperature range of 70–350 K.

Fig. 1 shows the semi-logarithmic forward current density–voltage (*J–V*) characteristics of an Ag/*p*-GaSe SBD in the temperature range of 70–350 K. It can clearly be seen from this figure that Ag/*p*-GaSe SBD has good rectifying properties at different temperatures and they are manifestly temperature dependent. Clearly, by decreasing the temperature, the *J–V* plots shift towards the higher bias region and a decrease of the current is observed as predicted by TE model. The *J–V* characteristics are linear in the semi-logarithmic scale over several orders of current, but deviate from linearity due to the effect of the interface states and serial resistance R_s, when the applied voltage is sufficiently large. Hence, detailed analysis of *J–V* characteristics is required to be taken into account the serial resistance effect for each temperature. Since it is the most reliable and sensitive method among several methods proposed in the literature for extracting

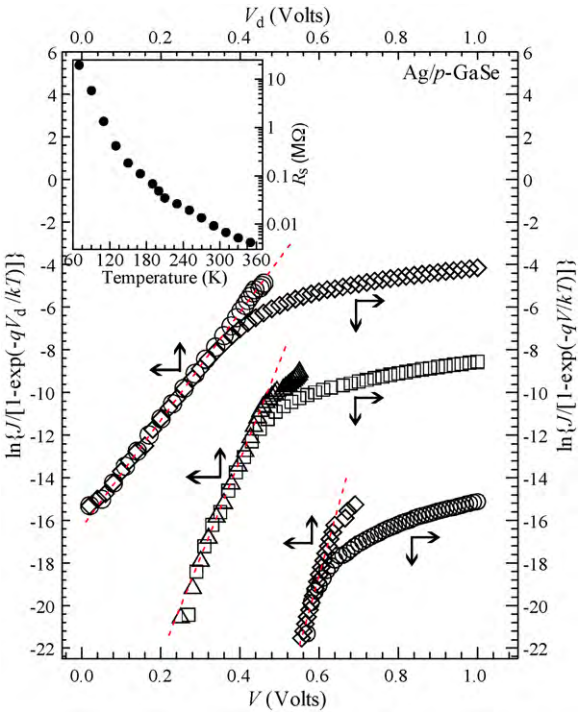

Fig. 2. Plots of the experimental $\ln[J/\{1-\exp(qV/kT)\}]$ vs. V and corrected $\ln[J/\{1-\exp(qV_d/kT)\}]$ vs. V_d curves considering the serial resistance R_s for 350, 200 and 70 K typical temperatures. Inset: Temperature dependence of the averaged serial resistance evaluated from the Cheung's functions.

the Schottky diode parameters when serial resistance is dominant and gets effective in all forward bias regions, a method was used suggested by Cheung and Cheung [24] and confirmed by Werner [44]:

$$\frac{dV}{d(\ln J)} = JA_{eff}R_s + n\left(\frac{kT}{q}\right) \quad (6)$$

$$H(J) = V - n\left(\frac{kT}{q}\right)\ln\left(\frac{J}{A^*T^2}\right) \quad (7)$$

where $H(J)$ can be written as:

$$H(J) = JA_{eff}R_s + n\varphi_{b0}. \quad (8)$$

Eq. (6) should give a straight line for the data of downward curvature in the forward bias J–V characteristics. Thus, a plot of $dV/d(\ln J)$ vs. J will give $A_{eff}R_s$ as the slope and nkT/q as the y-axis intercept. Using the n value determined from Eq. (6) and the data of downward curvature region in the forward bias region in Eq. (7), a plot of $H(J)$ vs. J according to Eq. (8) will also give a straight line with the y-axis intercept equal to $n\varphi_{b0}$. The slope of this plot also provides an alternative determination of R_s that can be used to check the consistency of Cheung's approach. Serial resistance calculated from Cheung functions have increased from 4.16 kΩ to 19.5 MΩ as temperature changing from 350 to 70 K. Temperature depended serial resistance of Ag/p-GaSe structure is shown in Fig. 2 as inset. As can be seen from this figure, the rapid increase of serial resistance cause variation steeply and limit the currents passing through the sample with decreasing temperatures in Fig. 1. Substantial values of the serial resistance at low temperatures are resulted from the bulk resistance, *i.e.* freeze out of the deep acceptors in the unintentionally doped GaSe [9,10,42,45,46]. As temperature lowered, free carriers are captured by the related deep acceptors located in the band gap and the GaSe exhibits semi-insulating behavior at low temperatures [45].

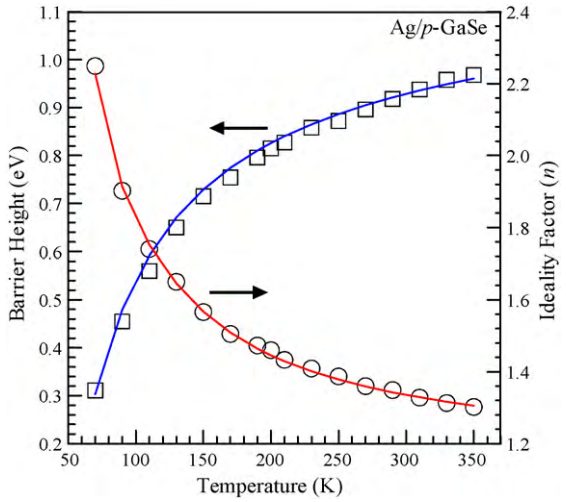

Fig. 3. Temperature dependence of the zero bias BH (the open squares) and the ideality factor (the open circles) for the Ag/p-GaSe Schottky contact according to DGD of BHs. The continuous curves show estimated values of φ_{ap} using Eq. (14) with $\delta_1 = 0.75$, $\bar{\varphi}_{01} = 1.21$ eV, $\sigma_{01} = 0.103$ eV, $\bar{\varphi}_{02} = 1.08$ eV and $\sigma_{02} = 0.097$ eV and n_{ap} using Eq. (15) with $\rho_{21} = 0.144$, $\rho_{22} = 0.220$, $\rho_{31} = -0.0058$ eV and $\rho_{32} = -0.0040$ eV, respectively.

For each temperature, the experimental J–V data is used to extract the serial resistance. Mean values of the determined serial resistances from Eqs. (6)–(8) are inserted in Eq. (1) and then by plotting $\ln[J/\{1-\exp(qV_d/kT)\}]$ vs. V_d plot, the ideality factor n and φ_{b0} at each temperature are extracted from the slopes and the y-axis intercepts, respectively. To illustrate that, representative plots of $\ln[J/(1-\exp(qV_d/kT))]$ vs. V_d at 350, 210 and 70 K for Ag/p-GaSe SBD are given in Fig. 2. As can be seen from Fig. 2, the J–V characteristics are linear in the semi-logarithmic scale over several orders of current at low forward bias as well, particularly at low temperatures. The experimental values of φ_{b0} and n range from 0.311 eV and 2.249 at 70 K to 0.968 eV and 1.302 at 350 K, respectively. Fig. 3 shows the temperature dependence of the BH and the ideality factor obtained by Eqs. (1) and (2) and Fig. 2. As seen in Fig. 3 both of the n (denoted by open circles) and φ_{b0} (denoted by open squares) are strongly temperature dependent and the ideality factor n increases with decreasing temperature while, the BH φ_{b0} decreasing.

Image-force lowering, tunneling through the barrier, an alteration of the charge distribution near the interface and/or generation-recombination in the depletion region are the phenomena routinely invoked as the reasons for these anomalies whereas, from my investigations on the combined effects of these process are not enough string to take into account for the measured fluctuations in the BH of Ag/p-GaSe SBD over most of the temperature region. These potential fluctuations have been attributed to a variety of causes including interface roughness due to non-uniform metal thickness and composition of the interface layer, grain boundaries, non-uniformity of interfacial charges, etc., [28,33,36,37,47].

On the other hand, the modified TE model that accounts inhomogeneous Schottky barriers has explained differences from conventional TE theory. Although conventional models treat the interface between the metal and the semiconductor as atomically flat and spatially homogeneous, it is recently established by ballistic electron emission microscopy (BEEM) that Schottky barriers have inhomogeneous area consisting of patches of relatively lower or higher barriers with respect to a mean BH $\bar{\varphi}_{b0}$ [48,49]. The total current is the sum of the currents through all of these patches and the whole junction area. Moreover, if the patch area is small (less than or comparable to the depletion region), the pinch-off effect should be taken into account, *i.e.* the effective reduction of the Schottky barrier height (SBH) between the patch and the sur-

rounding area is smaller than its original drop in the MS interface [31,32,38].

In the literature, both currents (through patches and the whole junction area) are usually assumed to be TE. As first introduced by Song et al. [28] at the moderate temperatures or in the large bias region at low temperatures, the combination of both currents can be approximately described by a GD of the SBH [36,37,41,50,51]. In this model, it is assumed that there are a number of parallel diodes having different SBH and every SBD can independently make contribution to the current so that the total current across the SBD with barrier inhomogeneities is composed of those flowing by all the individual patches through its own area and SBH as expressed in Eq. (1) but with an apparent BH and an apparent ideality factor, both of which are temperature dependent.

If a normalized GD function $P(\varphi_b)$ is introduced to describe the inhomogeneity of SBH, Eq. (1) is modified as the sum of the current flowing through all the micro-contacts with various BHs [1,28,36,37,41,50,52]:

$$J(V) = A^*T^2\left[\exp\left(\frac{qV_d}{nkT}\right)-1\right]\int_{-\infty}^{\infty}P(\varphi_{b0})\exp\left(-\frac{q\varphi_{b0}}{kT}\right)d\varphi_{b0}$$
$$= J_0\left[\exp\left(\frac{qV_d}{n_{ap}kT}\right)-1\right] \quad (9)$$

with

$$J_0 = A^*T^2\exp\left(-\frac{\varphi_{ap}}{kT}\right). \quad (10)$$

where φ_{ap} and n_{ap} are called as apparent BH and apparent ideality factor, respectively and

$$P(\varphi_{b0}) = \sum_{i=1}^{N}\frac{\delta_i}{\sigma_{0i}\sqrt{2\pi}}\exp\left[-\frac{(\bar{\varphi}_{b0i}-\varphi_{b0})^2}{2\sigma_{0i}^2}\right] \quad (11)$$

is the GD function where δ_i represent weight, σ_{0i} standard deviation and $\bar{\varphi}_{b0i}$ the mean BH value of the ith GD function. The normalization of $P(\varphi_{b0})$ requires $\sum_i\delta_i = 1$. Then, the relationship of φ_{ap} vs. $1/T$ can be deduced for an inhomogeneous SBD with multiple GD of BH [1,52]:

$$\varphi_{ap} = \frac{kT}{q}\ln\sum_{i=1}^{N}\delta_i\exp\left[\frac{q\bar{\varphi}_{b0i}}{kT}-\frac{1}{2}\left(\frac{q\sigma_{0i}}{kT}\right)^2\right] \quad (12)$$

and from Eq. (12), the following well-known formula can be obtained for $N = 1$.

$$\varphi_{ap} = \bar{\varphi}_{b0} - \frac{q\sigma_0^2}{2kT}. \quad (13)$$

If the BH distribution can be described with a Gaussian function, the plot of apparent BH against the inverse of the absolute temperature should follow a straight line giving σ_0^2; $\bar{\varphi}_{b0}$ from the slope and the intercept, respectively. Fig. 4 shows the φ_{ap} and n_{ap} vs. $q/2kT$ plots. As shown in Fig. 4, the apparent BH φ_{ap} displays two linear regions with different slopes over the temperature ranges 180–350 and 70–180 K. The values of 1.203 and 0.119 eV for $\bar{\varphi}_{b01}$ and σ_{01} and 1.072 eV and 0.097 eV for $\bar{\varphi}_{b02}$ and σ_{02} were obtained from the least square linear fitting to the experimental data in these regions, respectively. The observations obtained above indicate the presence of two GDs that is fairly differing from each other. Therefore, the double Gaussian distribution (DGD) should be introduced for better understanding of the problem [27,29,34,53,54]. Eq. (12) can be rearranged by considering of the DGD function for the BHs[1,52]

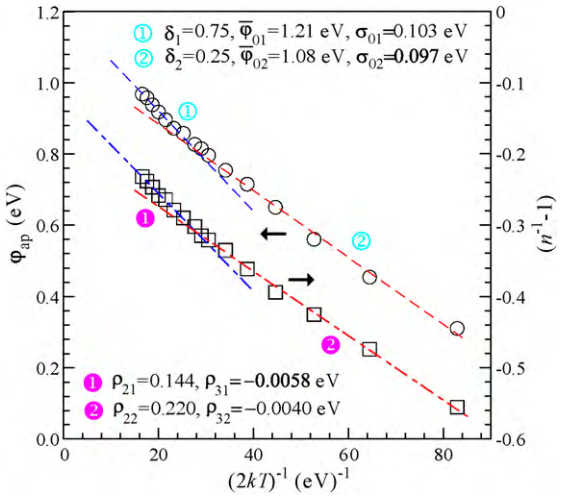

Fig. 4. Apparent BH φ_{ap} (the open circles) and apparent ideality factor n_{ap} (the open squares) vs. $q/2kT$ curves of the Ag/p-GaSe Schottky contact according to DGDs of BHs. Both of the data display two linear regions with different slopes over the temperature ranges 70–180 and 180–350 K. The dashed and dashed-dotted lines were obtained using Eqs. (14) and (15), where $\delta_1 = 0.75$, $\bar{\varphi}_{01} = 1.21$ eV, $\sigma_{01} = 0.103$ eV, $\bar{\varphi}_{02} = 1.08$ eV, $\sigma_{02} = 0.097$ eV and $\rho_{21} = 0.144$, $\rho_{31} = -0.0058$ eV, $\rho_{22} = 0.220$, $\rho_{32} = -0.0040$ eV, respectively.

as:

$$\varphi_{ap} = \frac{kT}{q}\ln\left[\delta_1\exp\left(\frac{q\bar{\varphi}_{01}}{kT}-\frac{1}{2}\left(\frac{q\sigma_{01}}{kT}\right)^2\right)+\delta_2\exp\left(\frac{q\bar{\varphi}_{02}}{kT}-\frac{1}{2}\left(\frac{q\sigma_{02}}{kT}\right)^2\right)\right]. \quad (14)$$

However, $(1/n_{ap}-1)$ vs. $q/2kT$ plot in Fig. 4 have also two linear regions with different slopes over the temperature ranges 180–350 and 70–180 K, respectively. Regarding the DGD function, apparent ideality factor n_{ap} can be expressed as [55] (see Appendix A):

$$\frac{1}{n_{ap}(V,T)}-1 = \frac{kT}{qV}\ln\left[\delta_1\exp\left\{\frac{q}{kT}\left(\frac{q\rho_{31}V}{2kT}-\rho_{21}V\right)\right\}+\delta_2\exp\left\{\frac{q}{kT}\left(\frac{q\rho_{32}V}{2kT}-\rho_{22}V\right)\right\}\right] \quad (15)$$

and from Eq. (15), the following well-known formula for the temperature dependent ideality factor can be obtained for $N = 1$:

$$\frac{1}{n_{ap}(V,T)}-1 = \frac{q\rho_3}{2kT}-\rho_2. \quad (16)$$

Therefore, by using the values of the $\bar{\varphi}_{01}$, σ_{01}, $\bar{\varphi}_{02}$, σ_{02} and δ_1 ($\delta_2 = 1-\delta_1$) as fitting parameters in Eq. (14) the φ_{ap} vs. $q/2kT$ plot can be obtained theoretically. The dashed lines in Fig. 4 were obtained using Eq. (14) for DGD of BH, where $\delta_1 = 0.75$, $\bar{\varphi}_{01} = 1.21$ eV, $\sigma_{01} = 0.103$ eV, $\bar{\varphi}_{02} = 1.08$ eV and $\sigma_{02} = 0.097$ eV. As can be seen, there is a good agreement the values of $\bar{\varphi}_{01}$, σ_{01}, $\bar{\varphi}_{02}$ and σ_{02} with the intercepts and slopes (1.203, 0.119, 1.072 and 0.097 eV) obtained from the least square fitting to the experimental data for two distinct regions, respectively. The standard deviation is a measure of the barrier homogeneity. When comparing $\bar{\varphi}_{01}$, σ_{01}, $\bar{\varphi}_{02}$ and σ_{02} parameters, it is seen that the difference between the mean values of these two GDs is about 0.12 eV and their standard deviations are ≈9% of the mean zero bias BH which indicate larger inhomogeneities at the interface of Ag/p-GaSe structure.

Moreover, as shown in Fig. 3, Eq. (14) fits very well to the experimental BH data φ_{ap} denoted by open squares with the $\delta_1 = 0.75$, $\delta_2 = 0.25$, $\bar{\varphi}_{01} = 1.21$ eV, $\sigma_{01} = 0.103$ eV, $\bar{\varphi}_{02} = 1.08$ eV and $\sigma_{02} = 0.097$ eV. The good agreement of the experimental data with

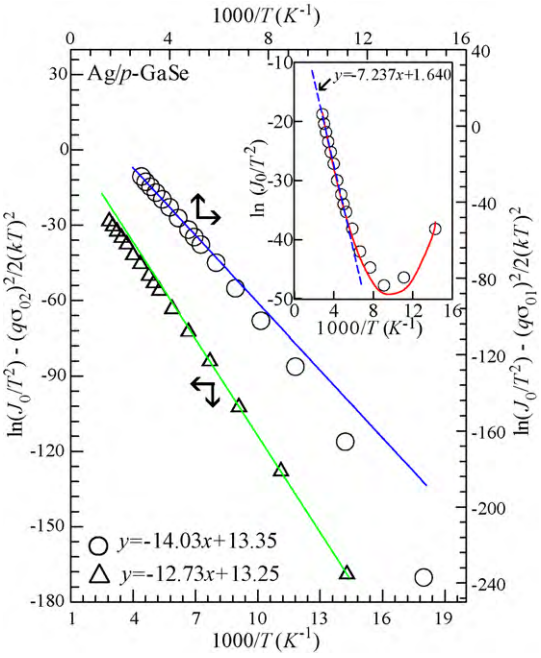

Fig. 5. Modified $[\ln(J_0/T^2) - (q^2\sigma_{0i}^2/2k^2T^2)$ vs. $1000/T]$ and conventional Richardson plots $[\ln(J_0/T^2)$ vs. $1000/T]$ (inset) for the Ag/*p*-GaSe Schottky diode according to DGDs of BHs. The open triangles and open circles represent the plots calculated with $\sigma_{01} = 0.103$ eV and $\sigma_{02} = 0.097$ eV, respectively. The straight solid lines indicate the best fitting of the data in the temperature ranges of 70–180 and 180–350 K. The continuous curve in the inset represents the data obtained using Eq. (17) with the parameters $\bar{\varphi}_{b01} = 1.209$ eV, $\bar{\varphi}_{b02} = 1.097$ eV, $\sigma_{01} = 0.103$ eV, $\sigma_{02} = 0.097$ eV and $A^* = 60\,\mathrm{A\,K^{-2}\,cm^{-2}}$.

the fitting curves in Fig. 3 indicates that the SBH inhomogeneity of our Ag/*p*-GaSe contact can be well described by a DGD model.

On the other hand, as can be clearly seen from Fig. 4, the plot of $(1/n_{ap} - 1)$ vs. $q/2kT$ should also possess different characteristics in the two temperature ranges because the diode contains double BH distributions. The linear behavior of this plot demonstrates that the ideality factor indeed expresses the voltage deformation of the GD of the Schottky BH.

In terms of Eq. (15) and by taking into account the values of the formerly obtained parameters δ_1, δ_2, $\bar{\varphi}_{01}$, $\bar{\varphi}_{02}$, σ_{01}, σ_{02} and ρ_{21}, ρ_{22}, ρ_{31}, ρ_{32} as fitting parameters, $(1/n_{ap} - 1)$ vs. $q/2kT$ plot denoted by dashed-dotted lines in Fig. 4 have been obtained theoretically for 180–350 and 70–180 K temperature ranges. The values of ρ_{21}, ρ_{31} and ρ_{22}, ρ_{32} are 0.144, −0.0058 eV for 180–350 K and 0.220, −0.0040 eV for 70–180 K range, respectively. As can also seen that there is a good agreement of ρ_{21}, ρ_{31} and ρ_{22}, ρ_{32} with the intercepts and slopes (0.119, −0.068 eV and 0.184, −0.045 eV) of the fitted lines obtained from the least square fitting to the experimental data for two distinct regions, respectively. Furthermore, as shown in Fig. 3, Eq. (15) fits very well to the experimental data of the ideality factor n denoted by open circles with the $\rho_{21} = 0.144$, $\rho_{22} = 0.220$, $\rho_{31} = -0.0058$ and $\rho_{32} = -0.0040$ eV values and formerly obtained fitting parameters (δ_1, δ_1, $\bar{\varphi}_{01}$, $\bar{\varphi}_{02}$, σ_{01} and σ_{02}).

As shown in Fig. 5, the conventional Richardson plot $[\ln(J_0/T^2)$ vs. $1000/T]$ deviates from linearity at low temperatures due to the barrier inhomogeneity as discussed above. The experimental data have a bowing at low temperatures and they appear to lie on a straight line above 180 K, yielding activation energy of 0.62 eV. The value of A^* obtained from the intercept of the straight portion at the ordinate is equal to $5.15 \times 10^{-4}\,\mathrm{A\,K^{-2}\,cm^{-2}}$. The value of A^* is much lower than both of the theoretically calculated and experimentally obtained values given in the literature for holes in *p*-type GaSe [43].

Since the conventional Richardson plot deviates from linearity at low temperatures due to the barrier inhomogeneity, it can be modified by combining Eqs. (10) and (12) as follows:

$$\ln\left(\frac{J_0}{T^2}\right) = \ln A^* + \ln\sum_{i=1}^{N}\delta_i \exp\left[-\frac{q\bar{\varphi}_{b0i}}{kT} + \frac{1}{2}\left(\frac{q\sigma_{0i}}{kT}\right)^2\right]. \quad (17)$$

Hence, modified Richardson plot $[\ln(J_0/T^2) - (q^2\sigma_{0i}^2/2k^2T^2)$ vs. $1000/T]$ according to Eq. (17) should also be a straight line with slope and intercept at the ordinate directly yielding the zero bias mean BH $\bar{\varphi}_{b0i}$ and A^*, respectively. The open circles and open triangles in Fig. 5 denote the modified Richardson plots obtained from the values of $\sigma_{01} = 0.103$ eV and $\sigma_{02} = 0.097$ eV, respectively. The least square linear fittings to these modified experimental data for 180–350 and 70–180 K ranges are depicted by solid lines in Fig. 5, which represent the true activation energy plots for the related temperature ranges, respectively. The calculations yielded zero bias mean BH $\bar{\varphi}_{b01}$ of 1.209 eV (in the range of 180–350 K) and $\bar{\varphi}_{b02}$ of 1.097 eV (in the range of 70–180 K). These values match exactly with the mean BHs obtained from the φ_{ap} vs. $q/2kT$ plot in Fig. 4. The intercepts at the ordinate give the Richardson constant A^* as $62.8\,\mathrm{A\,cm^{-2}\,K^{-2}}$ (in 180–350 K range) and $56.8\,\mathrm{A\,cm^{-2}\,K^{-2}}$ (in 70–180 K range). The obtained A^* values for two distinct ranges are in close agreement with the known value of $60\,\mathrm{A\,cm^{-2}\,K^{-2}}$ for *p*-type GaSe [42]. Furthermore, the recreated conventional Richardson plot by using Eq. (17) (denoted by solid curve) with the above parameters obtained is correlate well with the experimental points as shown in Fig. 5.

4. Conclusion

The above results suggest that strong variations of basic diode parameters for the Ag/*p*-GaSe Schottky structure with temperature could not be fully explained by considering the combined effects of tunneling, recombination, image-force lowering and serial resistance. Considering the BH inhomogeneity in the data analysis, single Gaussian model could not also satisfactorily explain the observed characteristics of the apparent BH and the ideality factor. However, the experimental *I–V* characteristics of the Ag/*p*-GaSe Schottky contact have been successfully interpreted based on a multiple GD model that assumes the simultaneous existence of the DGDs of the BH at the MS interface in the temperature range of 70–350 K. The temperature range has been limited by each straight line suggests the regime where the corresponding distribution is satisfactorily effective. Namely, φ_{ap} and n_{ap} vs. $q/2kT$ plots have two straight lines with negative slopes. The modified Richardson plots from the barrier inhomogeneity model with DGDs give zero bias mean BH $\bar{\varphi}_{b01}$ of 1.209 eV (in the range of 180–350 K) and $\bar{\varphi}_{b02}$ of 1.097 eV (in the range of 70–180 K). These values match exactly with the mean BHs obtained from the φ_{ap} vs. $q/2kT$ plot in the respective temperature ranges. Furthermore, it is seen that the modified activation energy plots yield for the Richardson constant A^* as 62.8 and $56.8\,\mathrm{A\,cm^{-2}\,K^{-2}}$ in the respective temperature ranges considering DGDs of the BH and exactly coincidence with the known value $60\,\mathrm{A\,K^{-2}\,cm^{-2}}$ for *p*-type GaSe. In conclusion, the experimental data of the Ag/*p*-GaSe Schottky diode can be satisfactorily explained by assuming the existence of DGDs of the BHs in the temperature range of 70–350 K, suggesting that the contacts are not spatially uniform.

Appendix A.

The ideality factor (n) is the result of the deformation of the spatial barrier distribution when a bias voltage is applied. The relationship between n and BH (φ_b) at a definite temperature and under

bias V is usually described within the thermionic emission theory as [36,37]:

$$\frac{1}{n_{ap}(V,T)} - 1 = -\frac{\Delta\varphi_b(V)}{V} \tag{A1}$$

with $\Delta\varphi_b(V) = \varphi_b(V) - \varphi_{b0}$.

As stated by Werner and Güttler in Ref. [36], Eq. (12) hold for all bias voltage V including $V = 0$ according to

$$\varphi_b(V) = \frac{kT}{q}\ln\sum_{i=1}^{N}\delta_i \exp\left[\frac{q\bar{\varphi}_{bi}(V)}{kT} - \frac{1}{2}\left(\frac{q\sigma_i(V)}{kT}\right)^2\right] \tag{A2}$$

$$\varphi_{b0} = \frac{kT}{q}\ln\sum_{i=1}^{N}\delta_i \exp\left[\frac{q\bar{\varphi}_{b0i}}{kT} - \frac{1}{2}\left(\frac{q\sigma_{0i}}{kT}\right)^2\right]. \tag{A3}$$

Hence, considering $\Delta\sigma^2(V) = \sigma^2(V) - \sigma_0^2$ [36], the change of the BH φ_b under bias yields from Eqs. (A2) and (A3) the result as

$$\begin{aligned}\Delta\varphi_b(V) &= \varphi_b(V) - \varphi_{b0} = \Delta\bar{\varphi}_b(V) - \frac{q\Delta\sigma^2(V)}{2kT} \\ &= \frac{kT}{q}\ln\left\{\frac{\sum_{i=1}^{N}\delta_i \exp\{q/kT[\bar{\varphi}_{bi}(V) - 1/2(q\sigma_i^2(V)/kT)]\}}{\sum_{i=1}^{N}\delta_i \exp\{q/kT[\bar{\varphi}_{b0i} - 1/2(q\sigma_{0i}^2/kT)]\}}\right\}.\end{aligned} \tag{A4}$$

From Eqs. (22a) and (22b) in Ref. [36]

$$\bar{\varphi}_{bi}(V) = \rho_{2i}V + \bar{\varphi}_{b0i} \tag{A5}$$

$$\sigma_i^2(V) = \rho_{3i}V + \sigma_{0i}^2 \tag{A6}$$

can be written for multi Gaussian distribution of BHs. Where, ρ_{2i} and ρ_{3i} are voltage coefficients of the mean BH and standard deviation, respectively. Hence, by combining of Eqs. (A4)–(A6) with Eq. (A1) and assume that $N = 2$ one then obtains Eq. (15).

References

[1] Y.L. Jiang, G.P. Ru, F. Lu, X.P. Qu, B.Z. Li, W. Li, A.Z. Li, Chin. Phys. Lett. 19 (2002) 553.
[2] P.A. Lee, Optical and Electrical Properties of Layered Materials, Reidel, Dordrecht, 1976.
[3] O. Lang, R. Schlaf, C. Pettenkofer, W. Jaegermann, J. Appl. Phys. 75 (1994) 7805.
[4] J.E. Palmer, T. Saitoh, T. Yodo, T. Tamura, J. Cryst. Growth 150 (1995) 685.
[5] S.M. Sze, Physics of Semiconductor Devices, Wiley, New York, 1981.
[6] J.F. Sánchez-Royo, A. Segura, V. Muñoz, Phys. Status Solidi A 151 (1995) 257.
[7] N.C. Ferneilus, Prog. Cryst. Growth Charact. 28 (1994) 275.
[8] B. Abay, H.S. Güder, Y.K. Yoğurtçu, Solid State Commun. 112 (1999) 489.
[9] J.F. Sánchez-Royo, A. Segura, A. Chevy, L. Roa, J. Appl. Phys. 79 (1996) 204.
[10] Y.K. Hsu, C.S. Chang, W.C. Huang, J. Appl. Phys. 96 (2004) 1563.
[11] G.B. Abdullaev, M.R. Akhundov, A. Akhundov, Phys. Status Solidi 16 (1966) 209.
[12] D.D. Askerov, A.M. Agaev, T.D. Dzhafarov, M.G. Ramazanzade, Phys. Status Solidi A 83 (1983) 323.
[13] G. Micocci, P. Siciliano, A. Tepore, J. Appl. Phys. 67 (1990) 6581.
[14] A.F. Qasrawi, Semicond. Sci. Technol. 21 (2006) 794.
[15] C. Tatsuyama, S. Ichimura, Jpn. J. Appl. Phys. 15 (1975) 843.
[16] W.C. Huang, S.H. Su, Y.K. Hsu, C.C. Wang, C.S. Chang, Superlattices Microstruct. 40 (2006) 644.
[17] B. Abay, Y. Onganer, M. Sağlam, H. Efeoğlu, A. Türüt, Y.K. Yoğurtçu, Solid State Electron. 41 (1997) 924.
[18] G. Çankaya, B. Abay, Semicond. Sci. Technol. 21 (2006) 124.
[19] H. Şafak, M. Şahin, Ö.F. Yüksel, Solid State Electron. 46 (2002) 49.
[20] B. Abay, G. Çankaya, H.S. Güder, H. Efeoglu, Y.K. Yogurtçu, Semicond. Sci. Technol. 18 (2003) 75.
[21] G. Çankaya, B. Abay, N. Uçar, H. Efeoğlu, Y.K. Yoğurtçu, Balkan Phys. Lett. (special issue) (2001) 64.
[22] E.H. Rhoderick, R.H. Williams, Metal–Semiconductor Contacts, Clarendon, Oxford, 1988.
[23] H. Rahab, A. Keffous, H. Menari, W. Chergui, N. Boussaa, M. Siad, Nucl. Instrum. Methods A 459 (2001) 200.
[24] S.K. Cheung, N.W. Cheung, Appl. Phys. Lett. 49 (1986) 85.
[25] J.R. Waldrop, R.W. Grant, Y.C. Wang, R.F. Davis, J. Appl. Phys. 72 (1992) 4757.
[26] C.I. Harris, S. Savage, A. Konstantinov, M. Bakowski, P. Ericsson, Appl. Surf. Sci. 184 (2001) 393.
[27] S. Chand, J. Kumar, Semicond. Sci. Technol. 11 (1996) 1203.
[28] Y.P. Song, R.L. Van Meirhaeghe, W.H. Laflére, F. Cardon, Solid State Electron. 29 (1986) 633.
[29] S. Chand, J. Kumar, Appl. Phys. A 63 (1996) 171.
[30] P. Cova, A. Singh, Solid State Electron. 33 (1990) 11.
[31] R.T. Tung, Phys. Rev. B 45 (1992) 13509.
[32] R.T. Tung, Mater. Sci. Eng. R 35 (2001) 1.
[33] V.W.L. Chin, M.A. Green, J.W.V. Storey, Solid State Electron. 33 (1990) 299.
[34] S. Chand, J. Kumar, Semicond. Sci. Technol. 10 (1995) 1680.
[35] R.T. Tung, J.P. Sullivan, F. Schrey, Mater. Sci. Eng. B 14 (1992) 266.
[36] J.H. Werner, H. Güttler, J. Appl. Phys. 69 (1991) 1522.
[37] J.H. Werner, H. Güttler, J. Appl. Phys. 73 (1993) 1315.
[38] J.P. Sullivan, R.T. Tung, M.R. Pinto, W.R. Graham, J. Appl. Phys. 70 (1991) 7403.
[39] R.F. Schmitsdrof, T.U. Kampen, W. Mönch, J. Vac. Sci. Technol. B 15 (1997) 1221.
[40] M.K. Hudait, S.B. Krupanidhi, Phys. B 307 (2001) 125.
[41] S. Zhu, C. Detavernier, R.L. Van Meirhaeghe, F. Cardon, G.P. Ru, X.P. Qu, B.Z. Li, Solid State Electron. 44 (2000) 1807.
[42] B. Abay, Ph.D. Thesis, Atatürk University Graduate School of Natural & Applied Science, 1994.
[43] C. Manfredotti, A.M. Mancini, R. Murri, A. Rizzo, L. Vasanelli, Nuovo Cimento B 39 (1977) 257.
[44] J.H. Werner, Appl. Phys. A 47 (1988) 291.
[45] B. Gürbulak, M. Yıldırım, S. Tüzemen, H. Efeoğlu, Y.K. Yoğurtçu, J. Appl. Phys. 83 (1998) 2030.
[46] H. Efeoğlu, T. Karacali, B. Abay, Y.K. Yoğurtçu, Semicond. Sci. Technol. 19 (2004) 523.
[47] S. Chand, Semicond. Sci. Technol. 17 (2002) L36.
[48] G.M. Vanalme, R.L. Van Meirhaeghe, F. Cardon, P. Van Daele, Semicond. Sci. Technol. 12 (1997) 907.
[49] G.M. Vanalme, L. Goubert, R.L. Van Meirhaeghe, F. Cardon, P. Van Daele, Semicond. Sci. Technol. 14 (1999) 871.
[50] S. Zhu, R.L. Van Meirhaeghe, C. Detaveriner, F. Cardon, G.P. Ru, X.P. Qu, B.Z. Li, Solid State Electron. 44 (2000) 663.
[51] I. Ohdomari, K.N. Tu, J. Appl. Phys. 51 (1980) 3735.
[52] Y.L. Jiang, G.P. Ru, F. Lu, X.P. Qu, B.Z. Li, S. Yang, J. Appl. Phys. 93 (2003) 866.
[53] S. Chand, J. Kumar, Appl. Phys. A 65 (1997) 497.
[54] A.F. Özdemir, A. Türüt, A. Kökçe, Semicond. Sci. Technol. 21 (2006) 298.
[55] B. Abay, M. Soylu, Y.K. Yoğurtçu, Sixth International Conference of the Balkan Physics Union, (BPU-6), İstanbul, Turkey, 2006, p. 693.